



Changes in cardiac proteome and metabolome following exposure to the PAHs retene and fluoranthene and their mixture in developing rainbow trout alevins

Andreas N.M. Eriksson^{a,*}, Cyril Rigaud^a, Anne Rokka^b, Morten Skaugen^c, Jenna H. Lihavainen^d, Eeva-Riikka Vehniäinen^a

^a Department of Biological and Environmental Science, University of Jyväskylä, P.O. Box 35, FI-40014, Finland

^b Turku Proteomics Facility, Turku University, Tykistökatu 6, 20520 Turku, Finland

^c Faculty of Chemistry, Biotechnology and Food Science, Norwegian University of Life Sciences, Campus Ås, Universitetstunet 3, 1430 Ås, Norway

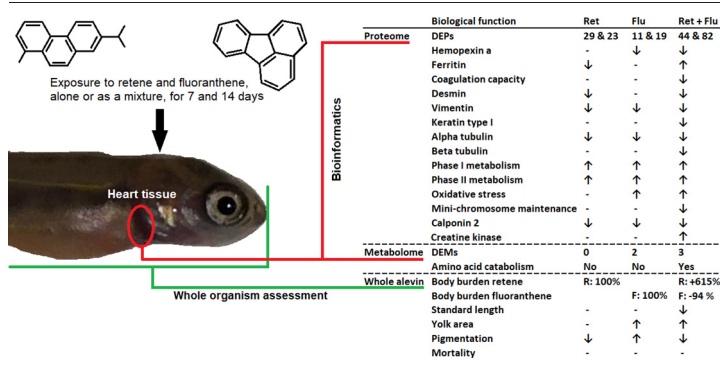
^d Umeå Plant Science Centre, Umeå University, KB. K3 (Fys. Bot.), Artedigränd 7, Fysiologisk botanik, UPSC, KB. K3 (B3.44.45) Umeå universitet, 901 87 Umeå, Sweden



HIGHLIGHTS

- Rainbow trout alevins were exposed to retene and/or fluoranthene for 7 and 14 days.
- PAH exposure resulted in treatment specific cardiac proteome and metabolome.
- Exposure specific phase II metabolism and body burdens profiles.
- Exposure to the binary mixture disrupted energy and iron metabolism.
- Impaired cellular integrity as per depletion of intermediate filaments and tubulins.

GRAPHICAL ABSTRACT



ARTICLE INFO

Article history:

Received 26 January 2022

Received in revised form 11 March 2022

Accepted 23 March 2022

Available online 26 March 2022

Editor: Daqiang Yin

Keywords:

PROTEOMICS

Metabolomics

PAH

Mixture

Developmental toxicology

Rainbow trout

ABSTRACT

Exposure to polycyclic aromatic hydrocarbons (PAHs) is known to affect developing organisms. Utilization of different omics-based technologies and approaches could therefore provide a base for the discovery of novel mechanisms of PAH induced development of toxicity. To this aim, we investigated how exposure towards two PAHs with different toxicity mechanisms: retene (an aryl hydrocarbon receptor 2 (Ahr2) agonist), and fluoranthene (a weak Ahr2 agonist and cytochrome P450 inhibitor (Cyp1a)), either alone or as a mixture, affected the cardiac proteome and metabolome in newly hatched rainbow trout alevins (*Oncorhynchus mykiss*). In total, we identified 65 and 82 differently expressed proteins (DEPs) across all treatments compared to control (DMSO) after 7 and 14 days of exposure. Exposure to fluoranthene altered the expression of 11 and 19 proteins, retene 29 and 23, while the mixture affected 44 and 82 DEPs by Days 7 and 14, respectively. In contrast, only 5 significantly affected metabolites were identified. Pathway overrepresentation analysis identified exposure-specific activation of phase II metabolic processes, which were accompanied with exposure-specific body burden profiles. The proteomic data highlights that exposure to the mixture increased oxidative stress, altered iron metabolism and impaired coagulation capacity. Additionally, depletion of several mini-chromosome maintenance components, in combination with depletion of several intermediate filaments and microtubules, among alevins exposed to the mixture, suggests compromised cellular integrity and reduced rate of mitosis, whereby affecting heart growth and development. Furthermore, the combination of proteomic and metabolomic data indicates altered energy metabolism, as per amino acid catabolism among mixture exposed alevins;

* Corresponding author at: P.O. Box 35, FI-40014 University of Jyväskylä, Finland.

E-mail addresses: andreas.n.m.eriksson@jyu.fi (A.N.M. Eriksson), cyril.c.rigaud@jyu.fi (C. Rigaud), anne.rokka@bioscience.fi (A. Rokka), morten.skaugen@nmbu.no (M. Skaugen), jenna.lihavainen@umu.se (J.H. Lihavainen), eeva-riikka.vehniainen@jyu.fi (E.-R. Vehniäinen).

plausibly compensatory mechanisms as to counteract reduced absorption and consumption of yolk. When considered as a whole, proteomic and metabolomic data, in relation to apical effects on the whole organism, provides additional insight into PAH toxicity and the effects of exposure on heart structure and molecular processes.

1. Introduction

Polycyclic aromatic hydrocarbons (PAHs) are a diverse group of pollutants of either natural or anthropogenic origin; the principal sources of the latter are industrial activities, urban sprawl and petroleum-related contamination (Behera et al., 2018; Pasparakis et al., 2019). Increased levels of PAH contamination has been linked to increased stress to the local environment and negative impacts on organismal health (Wickström and Tolonen, 1987; Kim et al., 2013; dos Santos et al., 2018). Newly hatched and developing fish larvae are especially sensitive to the influence PAH(s); symptoms of PAH toxicity include yolk sac and pericardial edema, spinal and craniofacial deformities, as well as hemorrhaging (these symptoms are referred to as blue sac disease (BSD) (Billiard et al., 1999)) and plausibly slower development (Eriksson et al., 2022). Yet, heart structure and function are especially sensitive to the influence of PAHs during early life development, as per improper development, and induction of bradycardia and arrhythmia (Incardona et al., 2004; Scott et al., 2011; Van Tiem and Di Giulio, 2011).

It is unclear exactly how exposure to PAH(s) induce developmental and cardiotoxicity in fish larvae. The best-known and most studied molecular pathway is the interaction between certain PAHs and subsequent activation of the aryl hydrocarbon receptor 2 (Ahr2), which in turn controls (among multiple processes) the induction of the cytochrome P450a1 (Cyp1a); a phase I xenobiotic metabolic enzyme (Köhle and Bock, 2007). Activation of phase I metabolism serves to increase the hydrophilicity of the substrate by addition of hydroxyl group(s), thus promoting further phase II metabolism and ultimately, excretion. This is perfectly exemplified by the stepwise metabolism of the PAH retene (Huang et al., 2017). Furthermore, developmental PAH toxicity is Ahr2 dependent, as knockdown of the *ahr2*, but not *cyp1a*, has been reported to prevent the formation toxicity in fish larvae (Incardona et al., 2006; Scott et al., 2011). Additional pathways governed by Ahr2 activation, such as cyclooxygenase-2, have also been suggested to contribute PAH mediated toxicity (Adverse Outcome Pathway 21 (Doering et al., 2019)). However, it has to be noted that not every PAH induce toxicity through improper activation of Ahr2. Rather, some PAHs induce toxicity non-specifically (narcosis), whereby the PAH induce cellular damages by impairing normal cell membrane function and disrupting ion homeostasis (Incardona et al., 2006; Meador and Nahrgang, 2019). However, the hypothesis of narcosis induced PAH toxicity has been questioned by Incardona (2017), who suggest that PAH-specific hydrophobicity, in relation to lipoproteins in the cell membrane, as the primary factor of non-specific PAH toxicity in fish larvae.

Two PAHs that can interact with, and activate Ahr2 signaling are retene and fluoranthene (Barron et al., 2004). Retene, also known as 1-methyl-7-isopropyl phenanthrene, is a common environmental pollutant, which is typically associated with effluents from pulp and paper industry, but also generated during forest fires, and by microbial degradation of resin acids, such as dehydroabietic acid (Leppänen and Oikari, 1999, 2001). The exact mechanisms by which retene induces toxicity in developing fish larvae are currently unknown, but activation of Ahr2 is required (Scott et al., 2011). In contrast, the PAH fluoranthene, which is a weaker Ahr2 agonist than retene (Barron et al., 2004), is a common component in crude oil and any mixture of PAHs (Baquer et al., 1988; Page et al., 1999). Mechanistically, fluoranthene can inhibit the function of Cyp1A by physically blocking the active site of the enzyme (Willett et al., 1998; Fent and Bättscher, 2000). Exposure to fluoranthene can therefore slow down its own metabolism, which in turn promotes temporal accumulation (Eriksson et al., 2022).

However, PAHs always occur as complex mixtures in the nature. Therefore, it is important to understand how complex and simple mixtures of PAHs induce toxicity at multiple levels of biological organization in developing fish larvae. The few controlled laboratory studies available have

reported potentized mixture toxicity relative to the components (Willett et al., 1998; Wassenberg and Di Giulio, 2004a, 2004b; Wills et al., 2009; Garner et al., 2013; Geier et al., 2018). This suggests that toxicity is induced through multiple simultaneous mechanisms and processes, all of which contribute to the induction of toxicity (Doering et al., 2019; Meador and Nahrgang, 2019).

In our previous studies on PAH-induced developmental toxicity, we observed that rainbow trout alevins (*Oncorhynchus mykiss*) exposed to the PAHs retene and fluoranthene (alone or as a mixture) (2022), or retene, pyrene and phenanthrene alone (2020a), developed unique cardiac transcriptomics, toxicity and body burden profiles. These results confirming the notion that PAHs toxicity is both compound, and potentially mixture-specific (Geier et al., 2018). Additionally, mixture toxicity could not have been predicted from the additive potential of the two components.

Even so, transcriptomic up-regulation does not necessarily result in an equally enriched protein expression (Vogel and Marcotte, 2012). It is unclear how exposure to a binary mixture of PAHs (with different mode of actions) would affect the cardiac proteome and metabolome, relative to the components, as no such study has been performed to the knowledge of the authors. Additionally, a number of studies on the proteomic and metabolomic responses in PAH exposed fish larvae report both species, developmental stage and compound specific alterations (Bohne-Kjersem et al., 2010; Elie et al., 2015; Doering et al., 2016; Rigaud et al., 2020b).

Therefore, the aims of this study were to investigate how the cardiac proteome and metabolome of newly hatched rainbow trout alevins responded to exposure, in vivo, to a binary mixture of retene and fluoranthene, relative to the components. Through such an approach, known mechanisms of toxicity could be validated, while unknown and novel mechanisms of cardiac toxicity could be discovered. We hypothesized that exposure to the individual PAHs, or the mixture, would generate unique cardiac proteomic and metabolomic profiles, in a similar fashion as was observed in our transcriptomic study (Eriksson et al., 2022). Investigating the cardiac metabolome could provide additional support to the alterations identified in the cardiac proteome and transcriptome. Therefore, by employing two different omic-approaches concurrently, in relation to developmental toxicity and PAH accumulation, it could be possible to shed new light on the impact of these pollutants on the underlying mechanisms of PAH induced cardiotoxicity in newly hatched and developing fish larvae.

2. Materials and methods

2.1. Exposure setup and maintenance

Alevins sampled for their cardiac proteome and metabolome are not from the same batch but exposed and sampled according to the same methodology, although 2.5 months apart. The cardiac proteome originates from the same alevins as those sampled for their cardiac transcriptome; for methodology and results, see Eriksson et al. (2022).

In short, newly hatched (<24 h) rainbow trout alevins (*Oncorhynchus mykiss*) were exposed semi-statically (water and chemicals were completely renewed on a daily basis) to dimethyl sulfoxide as control (DMSO), retene ($32 \mu\text{g}\cdot\text{l}^{-1}$), fluoranthene ($50 \mu\text{g}\cdot\text{l}^{-1}$) or the binary mixture of the two PAHs. The 360-degree-days old alevins were obtained from Hankatimen, Hankasalmi, Finland. Stock solutions were prepared by dissolving each PAH in pure DMSO. Chemical parameters and information are presented in Table 1. Nominal exposure concentrations were selected to induce toxicity, but not mortality, as per previous studies (retene) (Billiard et al., 1999; Vehniäinen et al., 2016) and preliminary testing (fluoranthene; ≤

Table 1

Exposure related information on stock solution concentrations (μM), volume of stock solution added per exposure bowl (μl), nominal exposure concentration (nM) of retene (Ret), fluoranthene (Flu) and the mixture (Mix), chemical purity (%), suppliers and CAS-numbers. Note: 136.6 nM of retene equals to $32 \mu\text{g l}^{-1}$, while 247.2 nM of fluoranthene equals to $50 \mu\text{g l}^{-1}$. Note that the volume of DMSO added to each exposure replicate is far below the upper limited of $100 \mu\text{g l}^{-1}$ recommended by the OECD (2013). NA = not applicable.

Exposure	PAH Stock solution concentration (μM)	Volume added (μl)	Nominal PAH exposure concentration (nM)	Purity (%)	Supplier	CAS Number
DMSO	Pure DMSO	20	NA	≥ 99.9	Sigma Aldrich	67–68-5
Ret + DMSO	13,655	10 + 10	136.6	98	MP Biomedical	483–65-3
Flu + DMSO	24,720	10 + 10	247.2	≥ 98	Sigma Aldrich	206–44-0
Mix	Same as above	10 + 10	136.6 + 247.2		[--- Same as above ---]	

$500 \mu\text{g l}^{-1}$ did not cause elevated mortality relative to DMSO exposed control, unpublished data).

Exposures were conducted in 1.5 l Pyrex glass trays, which had been pre-saturated for 24 h prior to the initiation of exposure with the corresponding chemicals. Every exposure replicate was filled with 1 l of filtered lake water (obtained at a depth of 6 m from Konnevesi Research Station, Central Finland; the levels PAHs in the water were negligible and below the level of detection of synchronous fluorescence spectroscopy (SFS)) and continuously aerated through glass Pasteur pipettes connected to an air pump. Alevins were exposed for and sampled after 7 and 14 days. The exposure (proteomics) which lasted for 7 days consisted of 12 replicates per treatment, while the 14 days exposure consisted of 8 replicates per treatment (proteomics; plus one additional replicate per treatment without alevins). The exposure meant for obtaining the cardiac tissue for metabolomics utilized 12 replicates per treatment, each containing 15 alevins, plus on set of trays without fish). At the start of the exposure, each replicate held 15 newly hatched and healthy rainbow trout alevins (free from signs of deformities). This corresponds to 720 and 480 alevins for the 7 and 14 days exposures, respectively.

Water temperature, measured daily, averaged $11.62 \pm 0.32 \text{ }^\circ\text{C}$, while a 16:8 light (from yellow fluorescent tubes) to darkness ratio was maintained throughout the exposure period. Any alevins found dead during exposure were recorded and assessed for symptoms of blue sac disease. Water quality (relative oxygen saturation ($> 100\%$), pH (7.16 ± 0.10) and conductivity ($26.83 \pm 4.35 \text{ mS m}^{-1}$)) of stock water were measured on Day 1, 3, 7, 10 and 14. The quality of the lake water (ammonium, alkalinity and Ca + Mg hardness) is considered as good, as per the Finnish Environment Institute (Hertta database; (Eriksson et al., 2022)). The concentration of PAH(s) in exposure water was assessed on the same days as water quality was checked. Five milliliters of exposure water, collected prior to the renewal of water and PAH(s), from 4 randomly selected tanks per treatment, were diluted 1:1 in ethanol (99.5% purity) and stored at $4 \text{ }^\circ\text{C}$ for later synchronous fluorescence spectroscopy analysis (results are presented in Table S1, while SFS methodology is presented in both Rigaud et al. (2020a) and Eriksson et al. (2022)).

At sampling, alevins were first photographed next to a millimeter scale paper and visually scored (0 or 1) for each symptom of blue sac disease investigated (hemorrhages, and yolk sac and pericardial edemas) according to standards set by Villalobos et al. (2000) and Scott and Hodson (2008). Alevins were decapitated using a scalpel blade, and the heart excised with forceps (Dumont #5, Fine Science Tools, Heidelberg, Germany). Hearts from 2 (Day 14) or 3 (Day 7) replicates were pooled in 1.5 ml microcentrifuge tubes ($N = 4$ per treatment with 30 (day 14) or 45 (day 7) hearts per N), snap frozen in liquid nitrogen and stored at $-80 \text{ }^\circ\text{C}$ for later proteomics analysis. In the case of cardiac metabolomics, sampled after 14 days of exposure, heart tissue from alevins of the same treatment, from 3 replicates, were pooled together (generating 4 replicates (N) per treatment; each replicate consisting of 45 hearts). The remaining carcasses were pooled based upon replicate in 1.5 ml microcentrifuge tubes for later body burden analysis ($N = 8$ per treatment; see Eriksson et al. (2022) or Rigaud et al. (2020a) for methodology).

2.2. Morphological analysis

Photographed alevins ($N = 18$ per treatment, 3 per replicate) were analyzed in silico using ImageJ (v1.51j8, National Institutes of Health, USA).

Using the millimeter scale as a known length reference, standard length and planar yolk area were measured. Pigmentation intensity of the lateral side and dorsal fin were assessed as a measurement of development (methodology described in Eriksson et al. (2022) and based upon Vernier's salmonid developmental catalog (Vernier, 1977)).

2.3. Proteomic analysis

Cardiac protein samples ($N = 4$ per treatment) were prepared following the extraction of RNA with TRI Reagent (Molecular Research Center, Cincinnati, OH, USA) as presented in Eriksson et al. (2022). Following the removal of the aqueous phase, ethyl-alcohol (99.5% purity) was added to precipitate DNA from the remaining organic and interphase, and the DNA was discarded. Proteins were then precipitated using isopropanol. The protein pellets were washed, first in 0.3 M guanidine hydrochloride (in 95% ethyl alcohol) and ethanol (99.5% purity). Finally, the proteins were dissolved using a solution of 8 M urea and 2 M thiourea in a 1 M Tris-HCl buffer (pH 8.0). Protein samples ($15 \mu\text{g}$) were reduced for 1 h using dithiothreitol ($37 \text{ }^\circ\text{C}$), then alkylated by iodoacetamide (1 h at room temperature) and the urea concentration diluted below 1 M using 50 mM Tris-HCl. By adding trypsin (1:30 w/w), protein samples were digested for 16 h at $37 \text{ }^\circ\text{C}$ and then desalted with SepPak C18 96-well plate (Waters, Milford, MA, USA) according to manufacturer's instructions and evaporated to dryness using a SpeedVac (Thermo Fisher Scientific) and dissolved in 0.1% formic acid before mass spectrometry (MS) analysis. The peptide concentrations were determined using a NanoDrop™ (Thermo Fisher Scientific) by measuring absorbance at 280 nm and the concentrations of every sample adjusted to $100 \text{ ng } \mu\text{l}^{-1}$.

The LC-ESI-MS/MS (Liquid Chromatography-Electrospray Ionization-Mass Spectrometry/ Mass Spectrometry) analysis and measurements were performed using a nanoflow HPLC system (Easy-nLC1200, Thermo Fisher Scientific) coupled to the Q Exactive HF mass spectrometer (Thermo Fisher Scientific) equipped with a nano-electrospray ionization source. The solutions containing cardiac peptides were first injected on to a trapping column and separated inline on a 15 cm C18 column ($75 \mu\text{m} \times 15 \text{ cm}$, ReproSil-Pur 5 μm 200 \AA C18-AQ, Dr. Maisch HPLC GmbH, Ammerbuch-Entringen, Germany). The mobile phase was constructed as follows: solution 1) de-ionized water spiked with 0.1% formic acid; and solution 2) was based upon an 80:20 mix of acetonitrile/water (v/v) with 0.1% formic acid added. Each run took 125 min; 85 min where solution 2 increased from 5% to 28% followed by an additional increase from 28% to 40% over 35 min. Finally, the samples were washed for 5 min with 100% solution 2 before the next run. This process was repeated twice for each sample as technical replicates.

2.4. Metabolomic analysis

2.4.1. Homogenization and metabolite extraction

The cardiac metabolome was analyzed, through untargeted metabolite profiling, in alevins exposed for 14 days. The same methodology was utilized by Rigaud et al. (2020b). In short: hearts from every alevin from 3 replicates of the same treatment were pooled (each pool thus contained 45 hearts), which equals 4 pooled replicates per treatment available for analysis. Cold methanol (CAS number: 67-56-1, Merck, Germany) with 0.1% of formic acid ($300 \mu\text{l}$; CAS number: 64-18-6, Sigma) and internal standard

solution (10 µl; 0.4 mg/ml of benzoic-d5 acid (CAS number: 1079-02-3, Sigma), 0.2 mg/ml of glycerol-d8 (CAS number: 7325-17-9, Sigma), 0.4 mg/ml of 4-methylumbelliferone (CAS number: 90-33-5, Sigma) in methanol) were added, and samples were homogenized with a bead mill (2 × 2 mm and 1 × 5 mm stainless steel beads, 2 × 15 s, 20 Hz, Qiagen TissueLyser II). The metabolites were extracted by vortexing the samples for 15 min at 4 °C. After a short centrifugation (2 min, 4 °C, 13500 × g), the supernatant was transferred to a fresh test tube and cold methanol (80% aqueous) with 0.1% formic acid (300 µl) was added, and samples were again vortexed for 15 min at 4 °C. Samples were then centrifuged (short program, as above), and the two supernatants combined. Aliquots (200 µl) were transferred to vials and dried in a vacuum at 35 °C for 40 min.

2.4.2. GC–MS analysis

Samples were derivatized by adding 50 µl (20 mg/ml) of methoxyamine hydrochloride (CAS number: 593-56-6, Sigma) in pyridine (CAS number: 110-86-1, VWR) at 37 °C for 90 min under continuous shaking (170 rpm). Samples were silylated with 50 µl of MSTFA (CAS number: 24589-78-4, Thermo Scientific) with 1% of TMSC (CAS number: 106018-85-3, Thermo Scientific) at 37 °C for 60 min under continuous shaking (170 rpm). Alkane series in hexane (5 µl; C7-C30) and 100 µl of hexane were added to each sample before GC–MS analysis.

GC–MS analysis was performed with an Agilent 7890A chromatography system coupled with an Agilent 7000 Triple quadrupole mass spectrometer and GC PAL autosampler and injector (CTC Analytics). For each run of analysis, 1 µl of sample was injected with pulsed splitless mode with a 30 psi pulse for 0.60 min and purge flow at 0.50 min in a single tapered liner with glass wool (Topaz 4 mm ID, Restek). Inlet temperature was set to 260 °C.

Helium flow in the guard column (Agilent Ultimate Plus deactivated fused silica, length 5 m, 0.25 mm ID) and in the analytical column (Agilent HP-5MS UI, length 30 m, 0.25 mm ID, 0.25 µm film thickness) was 1.2 ml min⁻¹ and purge flow was 46 ml min⁻¹. Helium flow in the restrictor column (deactivated silica, length 1.5 m, 0.15 mm ID) was 1.3 ml min⁻¹. MSD interface temperature was 280 °C, MS source 230 °C and quadrupole 150 °C. The oven temperature program was set at: 50 °C for 3 min, 7 °C min⁻¹ ramp to 240 °C, 10 °C min⁻¹ ramp to 330 °C, 2 min at 330 °C and post-run at 50 °C for 4 min. Mass spectra were collected with a scan range of 55–550 *m/z*.

AMDIS (version 2.68, NIST) and Metabolite Detector (versions 2.06 beta and 2.2 N (Hiller et al., 2009)) were used for deconvolution, component detection and quantification. Metabolite levels were calculated using the internal standard, benzoic-d5 acid, in relation to both normalized metabolite peak, and dry and fresh weight of the sample. Metabolites were annotated based on spectra and retention index matched to reference compounds and the Golm Metabolome database (GMD) (Hummel et al., 2007), NIST Mass Spectral database (version 2.0, Agilent) and Fiehn library (Agilent).

2.5. Bioinformatics

The raw proteomics output, from LC-ESI-MS/MS, was processed for protein identification and label-free quantification using MaxQuant (v1.6.2.3) (Cox and Mann, 2008). MaxQuant allowed for the assignment of proteins to their respective RefSeq codes for both *O. mykiss* and Atlantic salmon (*Salmo salar*) through the integrated Andromeda search engine (Cox et al., 2011). In short: the MaxQuant derived output was exported to, and analyzed, using the Perseus platform (v1.6.14.0) (Tyanova et al., 2016). Data was log₂-adjusted, filtered and protein (UniProt) annotations for Atlantic salmon, due to the better coverage compared to rainbow trout, added (obtained from datashare.biochem.mpg.de). Proteins with a significantly different abundance, compared to control, were identified using the built-in ANOVA + Tukey's post hoc test function, and the data output exported to Excel for manual sorting, analysis and comparisons.

Each differently expressed protein's (DEP) UniProt code was translated to the equivalent zebrafish gene symbol (obtained at zfin.org). Gene

ontology (GO) term and KEGG pathway over-representation analysis was performed using the online platform Metascape (Zhou et al., 2019). Identified terms and pathways were considered over-represented if both the *p* and *q*-value were ≤ 0.05.

The proteomic dataset is available through the repository service PRIDE, and accessible under the project code: PXD026443.

2.6. Statistics

Every statistical test, unless stated otherwise, was performed in R-studio (v1.2.5042), with significance cut-off set at *p* ≤ 0.05. The effects of exposure on mortality and pigmentation intensity (in relation to control) were analyzed using Fisher's exact test. As neither standard length nor planar yolk area were normally distributed (as per Shapiro-Wilk's test), Kruskal-Wallis test combined with Dunn's post hoc test, combined with Bonferroni's adjustment method, was employed. Due to the low *N* (4) per treatment, enrichment or depletion of metabolites, relative to control, were assessed using Mann-Whitney's *U* test corrected for multiple comparisons using the Bonferroni's adjustment method. Principal Component Statistical analysis of the cardiac metabolome was performed using Simca P⁺ (version 16, Umetrics) but visualized using R-studio.

3. Results and discussion

3.1. Mortality and morphology

The exposure of newly hatched and developing rainbow trout alevins to retene and fluoranthene (alone or as a mixture) did not significantly affect mortality; be that in relation to control or between the PAH treatments (*p* > 0.05; Table 2). This was expected as the concentrations of the PAHs were selected as to avoid elevated mortality (based upon preliminary experiments and previous studies (Billiard et al., 1999; Vehniäinen et al., 2016); for SFS quantified exposure concentrations, see Table S1). Measurement of actual exposure concentrations, sampled just before renewal of water and chemicals, yielded similar results (percentage of nominal concentration), as those reported in Eriksson et al., 2022.

Morphologically, alevins sampled for their cardiac metabolome presented similar alterations as observed among alevins sampled for their

Table 2

Summary of mortality (percentage, ± 95% confidence interval) and morphological endpoints (mean ± s.d.) in 14 days old rainbow trout alevins exposed to control (DMSO), retene (Ret), fluoranthene (Flu) or the binary mixture of the two (Mix). Dorsal fin- and yolk sac pigmentation intensity and mortality were assessed using Fisher's exact test, while standard length and yolk area were analyzed using Kruskal-Wallis' test combined with Dunn's post hoc test. Significant differences with regards to the standard length and planar yolk area are denoted using different Latin letters (lower and uppercase, respectively). In contrast, differences in pigmentation are denoted by different Greek letters and numbers, respectively. Note: these results are only representative for the alevins sampled for their cardiac metabolome. For results on alevins sampled for their cardiac proteome, see Eriksson et al. (2022).

Treatment	Mortality (%) [#]	Morphological [‡]		Pigmentation [‡]	
		Standard length (mm)	Planar yolk area (mm ²)	Dorsal fin (%)	Lateral side (%)
DMSO	3.89 (1.07–7.71)	22.76 ± 1.24 ^a	8.75 ± 4.14 ^{AB}	100% ^α	61% ¹
Ret	1.11 (0–3.98) ^Δ	22.44 ± 1.13 ^{ab}	7.51 ± 1.88 ^A	100% ^α	17% ²
Flu	3.89 (1.07–7.71)	22.43 ± 1.12 ^{ab}	10.08 ± 2.63 ^B	89% ^β	83% ³
Mix	1.11 (0–3.98) ^Δ	21.58 ± 1.11 ^b	9.99 ± 3.64 ^{AB}	78% ^β	11% ²

[#] *N* = 180 per treatment and 15 per replicate.

[‡] *N* = 18 per treatment and 3 per replicate.

^Δ True 95% confidence interval is –6.68 to +3.98; lowest limit is set to 0 as mortality cannot be negative.

cardiac transcriptome and proteome, after 14 days of exposure (Eriksson et al. (2022)). Nevertheless, and among alevins sampled for their cardiac metabolome, no reduction in standard length was observed following exposure to retene for 14 days (significantly reduced standard length was observed among retene exposed alevins sampled for their cardiac proteome and transcriptome; Eriksson et al. (2022)) or fluoranthene (not affected in either study). Alevins exposed to the binary mixture were significantly shorter and presented a significantly greater planar yolk area than control. Similar results, with regards to standard length, but not planar yolk area, were observed among alevins sampled for their cardiac transcriptome and proteome (Eriksson et al. (2022)).

An interesting aspect on the impact of exposure upon growth and development was the observation of hypopigmentation of the lateral side among retene and mixture exposed alevins and hyperpigmentation among fluoranthene exposed alevins, relative to control. Pigmentation of the dorsal fin on the other hand was significantly reduced among fluoranthene and mixture exposed alevins, but not retene, relative to control. These results are relatively similar to those reported by Eriksson et al. (2022), albeit variation exist. It is therefore plausible that pigmentation is influenced by seasonality and batches differences. Further assessment of pigmentation as an endpoint, in relation to exposure, seasonality and batch quality is required before any definitive conclusion can be established.

The combined results on the impact of exposure upon growth and pigmentation suggests that mixture exposed alevins might be at an earlier developmental stage at sampling, rather than just being shorter, compared to control alevins (Table 2), as pigmentation is, to a certain degree, controlled by Ahr activation in fish (Zodrow and Tanguay, 2003). It is also possible that retene exposed alevins were at an earlier developmental stage as well, based upon pigmentation intensity. What exactly caused the reduction in developmental gain and growth is unknown, although multiple processes are likely to be involved. The most plausible underlying processes are related to the reallocation of energy expenditures, plausibly away from growth and development to xenobiotic metabolism (Yue et al., 2021), potentially impairment of heart function (Vehniäinen et al., 2019; Ainerua et al., 2020) and structure (Incardona et al., 2011), which subsequently translates into a weakened cardiac output (Incardona, 2017), reduced absorption of yolk and fatty acids (Sorhus et al., 2021), circulation of nutrients and gas exchange. Significantly elevated pigmentation of the lateral side among fluoranthene exposed alevins (compared to control), in contrast, is plausibly a consequence of increased body burden and therefore, a potentially stronger Ahr-activation (Table 4).

3.2. Proteomic responses

3.2.1. General findings

The cardiac proteome, just like the cardiac transcriptome, responded in an exposure-specific manner to the influence of PAHs during early life development; similar results were reported by Rigaud et al. (2020a, 2020b). In total, 65 and 82 DEPs were identified after 7 and 14 days of exposure, respectively. Filtered per treatment, fluoranthene affected 11 and 19 proteins on Day 7 and 14; retene: 29 and 23; mixture: 44 and 82 (Fig. 1a and b; Tables s2 and s3). Interestingly, exposure to fluoranthene did not result in any unique DEP(s) by Day 7, while exposure to retene produced 20, and the mixture 29 unique expressions (Fig. 1a). Nevertheless, 3 DEPs were shared between the different PAH treatments on Day 7: Cyp1a (enriched relative to control; ↑), tubulin alpha chain (depleted relative to control; ↓) and methylosome subunit pICln (↓). No unique cardiac DEPs were identified among fluoranthene and retene exposed alevins sampled after 14 days, while exposure to mixture induced 47 unique DEPs (Fig. 1b). Seven DEPs were shared between the different treatments relative to control: one uncharacterized protein (†), Cyp1a (↑), UDP-glucuronosyltransferase (†), vesicle amine transport 1 (†), vimentin (↓), protein 4.1 isoform X5(↓) and 60S ribosomal protein L22 (↓). When the cardiac proteomes were compared between alevins sampled after 7 and 14 days of exposure, 24 shared DEPs were identified: exposure to fluoranthene resulted in 3 shared DEPs between Day 7 and 14, retene 4 and mixture 23 (Table s3).

Following bioinformatic analysis of the DEPs, and by Day 7, no over-represented pathways or terms were identified among alevins exposed to fluoranthene (every p and q-value >0.05), while exposure to retene caused the over-representation of plasma lipoprotein assembly (R-DRE-8963898; Tables 3 and s5). In contrast, exposure to the mixture over-represented xenobiotics metabolism (dre00980) and DNA replication (GO:0006267). After 14 days of exposure, fluoranthene over-represented the xenobiotic metabolism pathway (dre00980; Table s6). Alevins exposed to retene did not over-represent any term or pathway. Exposure to the mixture gave rise to a broader over-representation profile, which encompassed xenobiotic metabolism, DNA replication, regulation of coagulation (GO:0050878), cell redox homeostasis (GO:0045454) and a few other terms, which to a large extent, overlapped with the coagulation GO-term (e.g., GO:0010466, GO:0031589 and GO:0072376).

3.2.2. PAHs body burden, proteins involved in PAHs metabolism

Exposure to the binary mixture of retene and fluoranthene resulted in different body burden profiles of the PAHs when compared to those developed among alevins exposed to the individual components. By Day 14, the

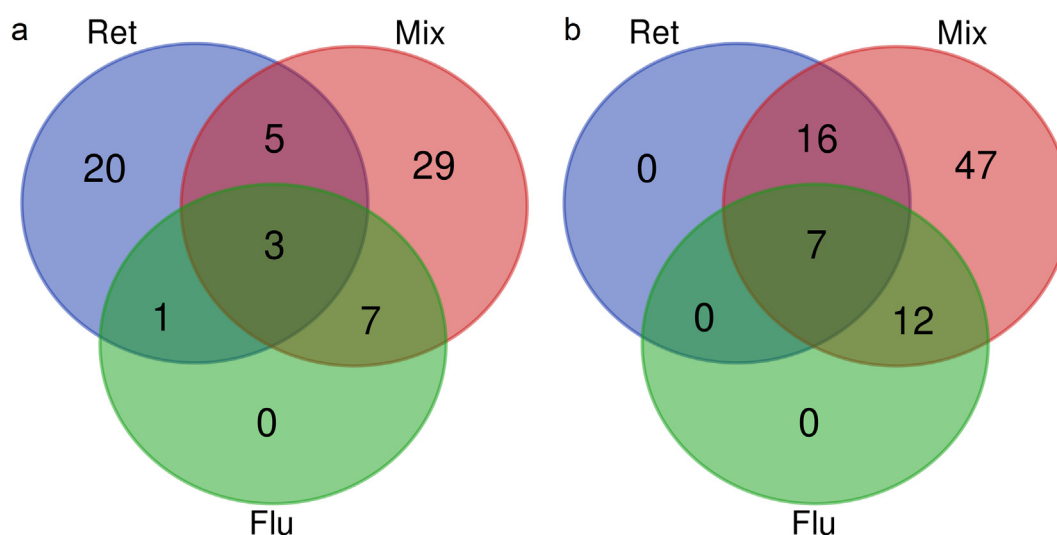


Fig. 1. Venn-diagram representations of differently expressed proteins following 7 (a) and 14 days (b) of exposure to retene (Ret), fluoranthene (Flu) and the binary mixture of the two PAH (Mix). The Venn-diagrams were created using the online tool provided by: <http://bioinformatics.psb.ugent.be/webtools/Venn/>.

Table 3

Over-represented GO-terms, as well as KEGG and reactome pathways, with a p and q-value ≤ 0.05 (as per Metascape) in rainbow trout alevins exposed to fluoranthene (Flu), retene (Ret) and the binary mixture of the two PAHs (Mix) and sampled after 7 and 14 days. For a detailed list of the depleted and enriched proteins governing these over-representations, see table s5 (Day 7) and s6 (Day 14), respectively. Note, in order to avoid reporting redundant pathways and terms, over-represented terms and pathways are those reported as “summary” by Metascape. For a complete list of over-represented terms and pathways, irrespective of q-value, see the file: Supplementary_file-Summary_Metascape.xlsx. NA = not applicable.

Sampled	Exposure	Term ID	Term description	p-Value	q-Value
Day 7	Flu		No over-representations identified		
	Ret	R-DRE-8963898	Plasma lipoprotein assembly	<0.0001	0.003
	Mix	dre00980	Metabolism of xenobiotics by cytochrome P450	<0.0001	<0.0001
Day 14		GO:0006267	pre-replicative complex assembly involved in nuclear cell cycle DNA replication	<0.0001	0.001
	Flu	dre00980	Metabolism of xenobiotics by cytochrome P450	<0.0001	0.018
	Ret		No over-representations identified		
	Mix	GO:0050878	regulation of body fluid levels	<0.0001	<0.0001
		GO:0010466	negative regulation of peptidase activity	<0.0001	<0.0001
		dre00980	Metabolism of xenobiotics by cytochrome P450	<0.0001	<0.0001
		GO:0045454	cell redox homeostasis	<0.0001	<0.0001
		GO:0006267	pre-replicative complex assembly involved in nuclear cell cycle DNA replication	<0.0001	0.002
		GO:0031589	cell-substrate adhesion	<0.0001	0.013
		GO:0072376	protein activation cascade	0.0001	0.037

body burden of retene had increased by 615%, while that of fluoranthene decreased by 94.4% in mixture exposed alevins compared to the body burden profiles of alevins exposed to the components (Table 4). These trends are in accordance with what was observed in our transcriptomic mixture study (Eriksson et al., 2022). These differences in body burden relates well to the exposure-specific up-regulation of proteins involved in xenobiotic metabolism. In total, eight DEPs known to be involved in phase I and II metabolism were identified among alevins exposed to the mixture: Cyp1a, UDP-glucuronosyltransferase (Ugt), 2 isoforms of sulfotransferase (Sult) and 4 isoforms of glutathione S-transferase (Gst). Furthermore, the mixture induced a stronger Cyp1a expression than the combined, additive effect of the components by Day 7, but not Day 14, as well as activation of a wider suit of phase II metabolic processes than the components. These exposure-specific differences in phase II metabolic responses confirm our previous transcriptomic findings on the relationship between the exposure-specific up-regulation of phase II metabolic processes and the corresponding body burden of the PAHs (Eriksson et al., 2022). Similar exposure-specific enrichment of phase I and II metabolic processes has been identified in the cardiac proteome of rainbow trout alevins exposed to retene, pyrene and phenanthrene individually (Rigaud et al., 2020b).

Interestingly, fluoranthene was detected and quantified in the cardiac metabolome among alevins exposed to fluoranthene alone, but below the limit of detection in the metabolome of alevins exposed to DMSO, retene and the binary mixture. This finding would imply that the fluoranthene, once absorbed, is distributed throughout the organism via the cardiovascular system. Alevins exposed to the mixture, by comparison, did not present detectable accumulation in heart tissue, whereby providing additional support to the notion of enhanced phase II metabolic capacity, and plausibly less uptake of fluoranthene in cardiovascular tissue.

Table 4

Average body burden of retene (Ret) and fluoranthene (Flu) per fish (\pm standard deviation) in 14 days old rainbow trout alevins exposed to the PAHs alone or as a binary mixture (Mix) and sampled for their cardiac metabolome. Body burden is background compensated. Statistically significant differences between the mixture and its components are denoted using lower and uppercase letters and established using Mann-Whitney's U test. N = 8 per treatment.

Treatment	Average retene body burden (pmol per alevins)	Average fluoranthene body burden (pmol per alevins)
Ret	1.77 \pm 0.48 ^a	0
Flu	0	3967 \pm 960 ^A
Mix	10.93 \pm 3.90 ^b	222 \pm 73 ^B

3.2.3. Iron metabolism and oxidative stress

Even though neither exposure over-represented any term or pathway related to iron metabolism, two DEPs essential for iron (Fe^{3+}) metabolism and homeostasis were identified in the cardiac proteome. These two proteins were hemopexin a (Hpxa; depleted by exposure to fluoranthene and the mixture on Day 7 and 14) and ferritin (depleted by retene on Day 7 and enriched by mixture on Day 7 and 14). Hemopexin is a plasma protein that efficiently sequesters free heme, thereby preventing oxidative damage to cells (Tolosano and Altruda, 2002). Depletion of hemopexin has previously been reported in both juvenile Atlantic cod (*Gadus morhua*) exposed to North Sea oil (Bohne-Kjersem et al., 2009), and in newly hatched rainbow trout alevins exposed to pyrene (Rigaud et al., 2020b). In humans, depletion of plasma hemopexin is clinically associated with an increase in circulating free heme, which in turn can be caused by ongoing hemolysis (Delanghe and Langlois, 2001). In contrast to hemopexin, ferritin has previously been observed to increase with increasing dose of oil (Troisi et al., 2007; Olsvik et al., 2012) or during anoxia (Larade and Storey, 2004). The primary function of ferritin is to store biologically available iron, making it non-reactive, as free and circulating iron is toxic and can act as a substrate for the formation of reactive oxygen species (Halliwell and Gutteridge, 1985). As the amount of circulating heme, normally, is maintained under strict homeostasis, there are two possible processes that could increase the concentration of circulating heme in plasma: leakage of newly produced and unbound heme, or following the dissociation from hemoproteins during oxidative stress (Sawicki et al., 2015). Hence, it seems plausible to assume that exposure to fluoranthene alone, or as part of a mixture, increased the rate at which hemopexin is depleted which in turn suggests increased availability of freely circulating heme (Delanghe and Langlois, 2001). However, the experimental protocol does not allow for the identification of the source of the free heme, but the effects of PAHs on erythrocytes should be investigated further.

As previously mentioned, un-scavenged free heme can aggravate oxidative stress by acting as a substrate for the generation of oxygen radicals (Halliwell and Gutteridge, 1985). We know from our transcriptomic dataset that exposure to fluoranthene and the binary mixture over-represented the GO-term oxidoreductase activity (GO:0016491) which involved the up-regulation of thioredoxin reductase 1, thioredoxin-like and peroxiredoxin 2 (Eriksson et al., 2022). Over-representation analysis of the cardiac proteome among mixture exposed alevins identified the GO-term cell redox homeostasis (GO:0045454), which suggests enrichment of anti-oxidative processes. Manual assessment of the involved genes revealed that exposure to the mixture enriched peroxiredoxin (also enriched by fluoranthene), peptide methionine sulfoxide reductase, thioredoxin reductase 1 and thioredoxin. These specific enrichments provide additional support to the possibility that fluoranthene and the mixture induced oxidative stress as part of the toxicity profiles and that it may take an extended exposure duration for

enrichment of certain proteins to reach detectable levels in the cardiac proteome. Furthermore, exposure-specific enrichment of anti-oxidative enzymes overlapped with the disrupted iron metabolism and homeostasis. It is unclear whether the oxidative stress is a consequence of, or exasperated by, increased amount of free and circulating heme; further studies on the relationship between PAH toxicity and oxidative stress is required.

Exposure for 14 days to the mixture, but not the components, resulted in the over-representation of the GO-term regulation of body fluid levels (GO:0050878; every protein involved in this term was depleted; Table S5). The functions of the involved proteins are primarily related to coagulation, as per the depletion of antithrombin, plasminogen, protein C (vitamin K-dependent) and fibrinogen (gamma chain-like). Combined, these depletions suggest impaired anti-coagulation regulation and capacity. This is further supported by the depletion of pro-coagulant proteins, such as von Willebrand factor (–like; VWF) and coagulation factor VIII (–like). During normal circumstances, the latter protein is always associated in an inactive form with the former, but dissociates and becomes active upon blood vessel injury, thus triggering clotting mechanisms (Zimmerman and Edgington, 1973; Weiss et al., 1977). Hence, depletion could indicate ongoing or past injuries to the cardiovascular system, which could in turn contribute to the formation of PAH induced cardiotoxicity. The negative effect of PAH(s) upon coagulation capacity has previously been reported in mummichog embryos (*Fundulus heteroclitus*) exposed to PAH-contaminated sediment extracts, as per an observed correlation between downregulation of *vwf* and cardiotoxicity (Bozinovic et al., 2021). However, the identification of abovementioned coagulation-related proteins is a novel finding, which could contribute to, or even aggravate cardiotoxicity. How and why exposure affected coagulation-related proteins is, however, unknown and requires further inquiry.

3.2.4. Proteomic responses in relation to cellular stability and proliferation

Several significantly altered proteins, involved in cellular integrity and proliferation, were identified following exposure to the PAHs. With respect to cellular proliferation, over-representation of DNA replication (dre03030) was observed in mixture exposed alevins sampled after both 7 and 14 days. This specific over-representation implies restricted DNA replication and cellular division at an early checkpoint, as per significant depletion of 4 components of mini-chromosome maintenance proteins (Mcm; type 4, 6, and 7 by Day 7; and type 5, 6 and 7 by Day 14). During normal conditions, the Mcm components form the pre-replication complex together with Cdc6 and Cdt1 proteins; a molecular complex that is essential for the initiation of DNA replication (Dutta and Bell, 1997; Cvetic and Walter, 2006). Depletion of several types of Mcm would thus suggest that exposure to this mixture restricted organ growth at an early molecular stage, which could potentially translate to smaller heart due to fewer rounds of cellular division. Reduced heart size and fewer cardiomyocytes have been observed before in developing rainbow trout (Hornung et al., 1999) and zebrafish (Antkiewicz et al., 2005) exposed to the dioxin TCDD (which also induces toxicity through Ahr2 agonism (Tanguay et al., 2003)). A decreased expression of *mcm2* has previously been reported in Atlantic cod larvae (*Gadus morhua*) exposed to weathered crude oil (Olsvik et al., 2012). Why and how depletion of abovementioned Mcm-components occurred are beyond the scope of this manuscript, but should be investigated further.

No over-representation related to cellular integrity was identified. However, assessment of the individual DEPs highlighted additional effects of exposure on processes related to cellular integrity and proliferation. The abundance of cardiac tubulin alpha- (all treatments on Day 7 but only mixture by Day 14) and beta chain proteins (mixture on Day 7 and 14) were found to be depleted relative to control. Together, the alpha- and beta tubulins form the basis of the cytoskeleton, the microtubules (Nogales, 2000). Depletion of tubulins has previously been linked to decreased rate of mitosis, as the alpha chain tubulin acts as the microtubule anchor during mitosis from which beta tubulins extend (Mitchison and Kirschner, 1984; Meunier and Vernos, 2012). Therefore, it is plausible that these depletions are in related to the depletion of Mcm-components.

The cytoskeleton stability and integrity were further affected by exposure, as per the depletion of keratin type I cytoskeletal 18 (–like), desmin

(–like) and Vimentin. Keratin type I cytoskeletal 18 (–type), which was depleted following exposure to the mixture, is a low molecular weight simple keratin, which together with keratin 8 (a type II keratin) form some of the most abundant intermediate filaments (Paramio and Jorcano, 2002). Altered abundance of keratin 18 could thus contribute to impaired cardiomyocyte structure following exposure to PAH, and thereby to altered heart morphology (Scott et al., 2011).

Desmin and vimentin, in contrast, are both type III intermediate filaments; the former was depleted following exposure to retene and the mixture, while the latter was depleted irrespective of exposure. Desmin is required for the maintenance of muscle structure and function, where it connects the myofibril to the Z-lines (Sequeira et al., 2014). The depletion of desmin draws attention to an interesting finding from our transcriptomic dataset: the down-regulated nebulin (*nebl*) by every PAH treatment (Eriksson et al., 2022). As a protein, Nebl is, together with desmin, important for the formation of the Z-line in heart musculature. Knockdown of *nebl* in mice is associated with broadening of the Z-line, but does not affect the lifespan (Mastrototaro et al., 2015). Hence, there is a good probability that exposure to PAHs altered the Z-line and therefore cardiac muscle morphology. What the consequences are for the heart is unknown, but the depletion could be either compensatory, as to offset altered action potential (Vehniäinen et al., 2019), or a direct effect of PAH(s) toxicity.

Vimentin (Vim), which is also a type III intermediate filament, serves to anchor organelles and allows for the cell to be dynamic and maintain structural cohesion (Katsumoto et al., 1990). It is unknown how (or even if) depletion of Vim contributed to PAH-induced cardiotoxicity. A previous study on *Vim*-null mice reported no changes in the structural phenotypes of multiple organs, nor did the lack of the *vim*-gene affect breeding capacity (Colucci-Guyon et al., 1994). The authors hypothesized that other intermediate filaments could compensate for the lack of *vim*/Vim. However, in our PAH exposed rainbow trout alevins, multiple cardiac intermediate filaments were depleted, and it is thus plausible that no such compensatory mechanisms can occur, and if they do, the compensatory mechanism would be limited, as several types of filaments are depleted, especially among mixture exposed alevins.

Additionally, we found that 7 days of exposure to the mixture, and every PAH treatment on Day 14, significantly depleted calponin 2 (*Cnn2*), which is one among many important factors involved in vascular development, cytoskeletal organization and heart function (Fukui et al., 1997; Tang et al., 2006). Knockdown of *cnn2* in zebrafish produces deleterious phenotypes as per increased occurrence of pericardial- and hindbrain edemas, while decreasing the heart rate and restricting the circulation of erythrocytes, and consequently resulting in high mortality rates (Tang et al., 2006).

Collectively, these abovementioned results suggest a decreased rate of cellular proliferation, as well as impaired cellular structure and stability. The depletion of abovementioned intermediate filaments, in combination with the down-regulation of *nebl*, alongside the known impact of PAHs on cardiac ion channels and subsequently altered repolarization of the action potential could all contribute to impaired heart morphology and function as well as overall cardiotoxicity. The slower growing and developing heart could cause downstream consequences for the whole organism as circulation of nutrients, oxygen and hormones becomes restricted (Incardona et al., 2009; de Soysa et al., 2012; Sørhus et al., 2017); factors that potentially could be related to slower development among mixture, and potentially retene, exposed alevins.

3.3. Metabolomic responses

Exposure to the PAH(s) alone, or as a mixture, resulted in few significantly impacted cardiac metabolites after 14 days of exposure, as per the untargeted metabolite profiling approach. Using principal component analysis (PCA), we found that components 1 and 2 explained 50.1% of the variation and thus highlighted a shift in the cardiac metabolome composition in PAH exposed alevins compared to control (Fig. 2a; fresh weight adjusted). In contrast, components 1 and 3 revealed that the cardiac metabolome composition among mixture exposed alevins were more akin to that of

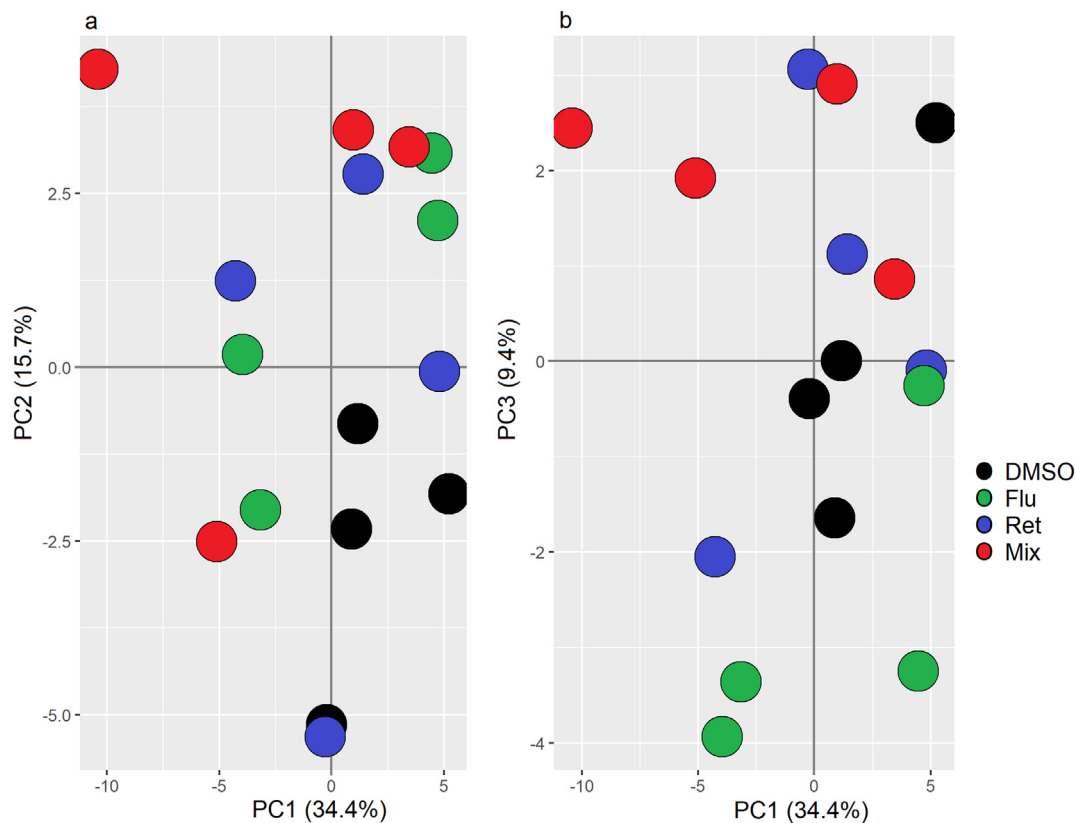


Fig. 2. Principal Component Analysis of the cardiac metabolome from 14-days old rainbow trout alevins exposed to either DMSO (black; control), retene (blue; Ret), fluoranthene (green; Flu) and the binary mixture of the two (red; Mix). Plot a) represents comparison between principal component 1 and 2 while b) the comparison between component 1 and 3. Results are compensated for fresh weight.

retene exposed alevins, than those exposed to fluoranthene (Fig. 2b). Metabolite levels, adjusted for dry weight, were excluded from the analysis due to an outlying control replicate, and poorer separation of the components (Figs. s1; s2a and s2b). Additionally and for the sake of simplicity, the impact of the mixture on energy metabolism in heart tissue (proteomics and metabolomics) is visualized in Fig. 3.

In total, 60 cardiac metabolites were detected, identified and annotated. However, three metabolites were omitted from analysis due to abundances being lower than the limit of detection in control. These were hypoxanthine, hydroxyfluorene and fluoranthene. Among the remaining 57 metabolites, 5 were found at significantly different abundance relative to control (Mann-Whitney with Bonferroni adjustment method). Exposure to retene did not significantly affect any metabolite relative to control. Fluoranthene enriched glucuronic acid and the sugar alcohol arabitol, while the binary mixture depleted methionine, putrescine and hypotaurine significantly, and phenylalanine near-to-significantly ($p = 0.0535$). By comparison, Rigaud et al. (2020b) did not observe any significantly impacted cardiac metabolite in rainbow trout alevins exposed to retene for 14 days, but among those exposed to pyrene and phenanthrene (albeit using a different statistical approach); exposure to the latter two PAHs altered the abundance of a minor number of metabolites: e.g. depletion of valine and alanine, which indicated amino acid catabolism. They also reported that exposure to phenanthrene enriched glucuronic acid and arabitol, just like fluoranthene; an observation that would suggest that these two PAHs affect similar type of processes. Decreased abundance of amino acids has also been observed in the metabolome of newly hatched zebrafish exposed to benz[*a*]anthracene (BAA) and its oxidized form (Elie et al., 2015).

Out of the 5 significantly and differently abundant metabolites, only one amino acid was observed at altered abundance: methionine, significantly depleted following exposure to the mixture. Depletion of methionine is plausibly a consequence of increased demand for cysteine (which is required in glutathione metabolism). The biotransformation is facilitated by the S-

Adenosyl methionine (SAM-e) cycle where methionine is metabolized in a three-step reaction to homocysteine, which can then be transformed to cysteine in two steps (Finkelstein and Martin, 2000) (Fig. 3). Depletion of hypotaurine among mixture exposed alevins could, just like methionine, could be linked to cysteine. During normal cellular functionality, taurine is produced from hypotaurine, which in turn is derived from cysteine. The amount of taurine in the cardiac metabolome was also (on average, but not significantly) depleted among mixture exposed alevins relative to control. Hence, the depletion of hypotaurine is plausibly linked to restrictions in the enzymatic conversion rate of cysteine, as the latter could be in demand for glutathione metabolism rather than the biosynthesis of taurine. Alternatively, cysteine can be catabolized following biotransformation to pyruvate. Hence, exposure-specific whole body quantification of cysteine, and other amino acids, could therefore shed additional light on these aspects.

The near-to-significant depletion of phenylalanine could imply ongoing amino acid catabolism. This notion is indirectly supported by data from our transcriptomic study (Eriksson et al., 2022), as exposure to the mixture caused up-regulation of tyrosine aminotransferase (*tat*; up-regulated on Day 3) and fumarylacetoacetate hydrolase (*fah*; up-regulated on Day 3, 7 and 14). The corresponding proteins are involved in the biotransformation of phenylalanine to tyrosine by *Tat* (Dietrich, 1992), which is then transformed into fumarate by *Fah* (Bateman et al., 2001). Fumarate, in turn, can be utilized in the citric acid cycle for the generation of both energy and reducing agents. The absence of enriched *Tat* and *Fah* proteins is most likely related to quantification rather than temporal aspects, especially since the heart is less metabolically active than other organs.

Furthermore, exposure to the mixture enriched four proteins essential in aerobic energy metabolism: phosphofructokinase (PFK), 2-oxoglutarate dehydrogenase (OGDC; also enriched by retene), dihydroliipoamide acetyltransferase (a component of the pyruvate dehydrogenase complex) and glucan phosphorylase (α -1,4). PFK is essential in the glycolysis as it catalyze the reaction: D-fructose 6-phosphate + ADP \rightarrow fructose 1,6-

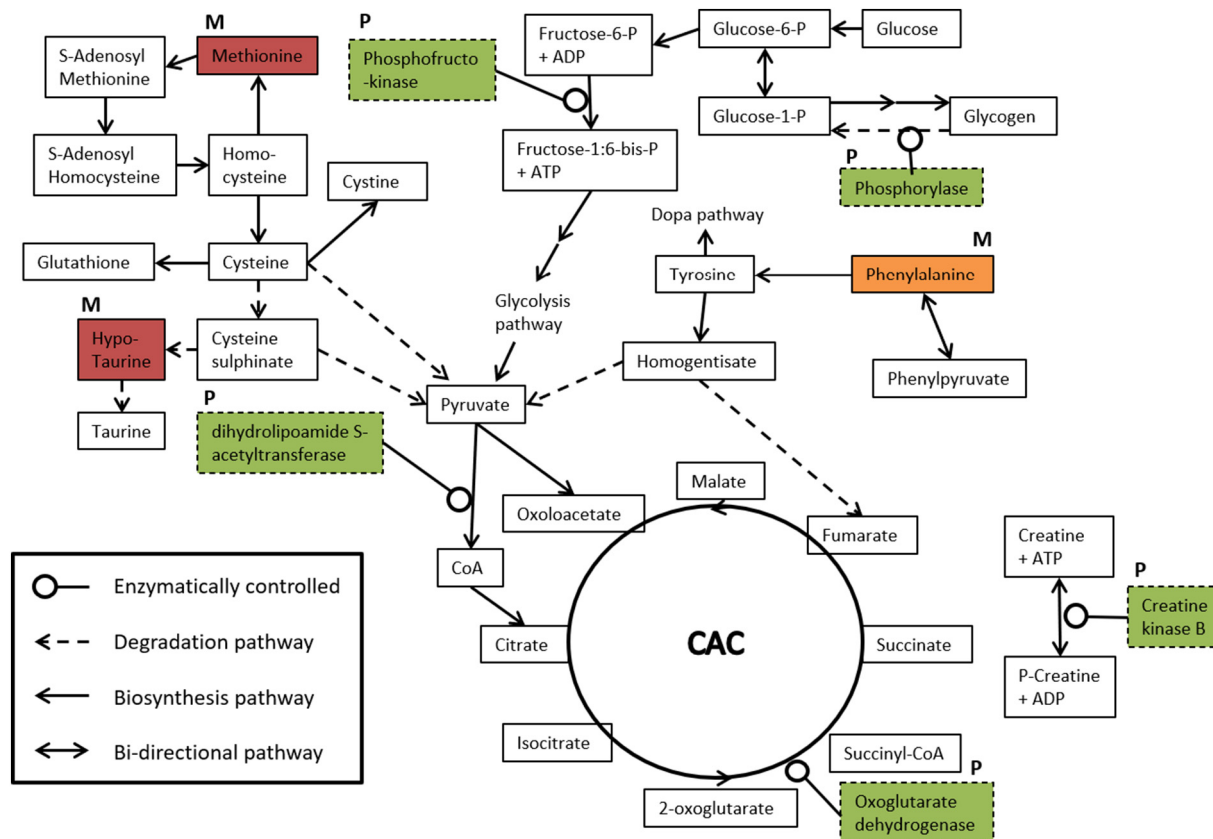


Fig. 3. A simplified visualization representing the impact of mixture on energy metabolism in heart tissue, as per the cardiac proteome (P) and metabolome (M). Boxes with a solid boarder represent products, while boxes with dashed boarders represent enzymes. Boxes colored in green indicate enrichments, while red and orange represent significantly and near-to-significant depletions, respectively. CAC = Citric Acid Circle.

bisphosphate + ATP (Uyeda, 1979). In contrast, OGDC catalyzes an essential reaction in the citric acid cycle: α -ketoglutarate + NAD^+ + Acetyl-CoA (CoA) \rightarrow Succinyl CoA + CO_2 + NADH (Williamson, 1979). Alpha-glucan phosphorylase on the other hand is involved in multiple biochemical reactions, including carbohydrate metabolism, as per UniProt. Enrichment of dihydrolipoamide acetyltransferase suggests increased rate of conversion of pyruvate to CoA, indicative of increased demand for energy.

Additional support for increased and altered metabolic activity is provided by the enrichment of creatine kinase B (– type). This enzyme facilitates the reversible and ATP/ADP dependent conversion of creatin \leftrightarrow phosphocreatine (PCr) (Oliver, 1955). Hence, PCr can be reverted back to creatin by the same enzyme and thus generate a localized burst of ATP, when required. Combined, the proteomic-, transcriptomic- and metabolomic data suggests that exposure to this mixture increases energy requirements, be that aerobically or catabolically (Fig. 3). However, and due to the poorer metabolic capacity of the heart, relative to the liver, these results on amino acid metabolism could indicate a systemic energy deficit in mixture exposed alevins rather than a localized deficit, as our data indicate. These results are especially relevant since heart tissue primarily utilize β -oxidation of fatty acids to cover energy expenses, rather than glycolysis and amino acid catabolism (Grynberg and Demaison, 1996).

Enrichment of arabitol and glucuronic acid following exposure to fluoranthene indicates either increased rate of formation, decreased rate of utilization or both. Arabitol is a sugar alcohol that can be utilized in energy metabolism through the pentose phosphate pathway (Bateman et al., 2001) (PPP). The primary outcome of PPP is the formation of NADPH, which in turn is important in multiple biological processes, including counteracting oxidative stress. Hence, enrichment could suggest that increased oxidative stress had occurred and that accumulation of arabitol could therefore be left-over material that can be utilized for the formation of NADPH from NADP^+ as well as maintaining the equilibrium between oxidized- and

reduced glutathione (Stanton, 2012). Glucuronic acid on the other hand is primarily utilized in phase II metabolism by UDP-glucuronosyltransferase (UGT). Exposure to fluoranthene induced a weak but statistically significant enrichment of UGT by Day 14 (a 64.9% stronger induction relative to control). It is possible that partial inhibition of Cyp1a by fluoranthene could limit the utilization of glucuronic acid and thus force its enrichment.

However, metabolomic investigations at earlier timepoints are required to confirm and assess the trends temporally. Furthermore, the low number of metabolomic replicates and material ($N = 4$ per treatment) limits the statistical analysis. It is likely that a greater number of replicates with more material per replicate could produce a more precise assessment of the impact of exposure on the cardiac metabolome. Likewise, sampling and assessment of other tissues, with higher metabolic capacity than cardiac tissue, could highlight other impacted metabolic pathways and processes.

4. Conclusion

We found that the exposure to retene, fluoranthene and their binary mixture produced exposure-specific toxicity profiles in newly hatched rainbow trout alevins with regards to development, growth and body burden, alongside exposure-specific cardiac proteome and metabolome profiles. Additionally, the effects exerted by the mixture on the growing and developing alevins could not be predicted from the additive effect of the components as only mixture exposed alevins were significantly shorter compared to control, while impacting a broader repertoire of cardiac proteins and pathways. Exposure-specific changes in the cardiac proteome, just like in the transcriptome (Eriksson et al., 2022), could explain the exposure-specific body burden profiles, as per PAH-specific induction of phase II metabolic processes and inhibition of Cyp1a by fluoranthene. When alevins were exposed to the mixture, a stronger and more diverse induction of phase I and II metabolic responses was observed which facilitated

decreasing body burden of fluoranthene, while the body burden of retene increased compared to the alevins exposed to the individual components. Exposure to the mixture increased the abundance of ferritin, while decreasing hemopexin (the latter was also depleted following exposure to fluoranthene) which would suggest disrupted iron metabolism and potentially increased oxidative stress. It is plausible that the altered iron metabolism is related to impaired coagulation as well as impacted erythrocyte cell membrane components. Exposure to the mixture caused decreased abundance of several components affecting cell proliferation and structure, and depletion of alpha and beta tubulin chains, which suggests impaired cellular integrity. This is further supported by depletion of several components of intermediate filaments that are involved in cell structure, vimentin and desmin for example. In contrast, analysis of the cardiac metabolome revealed few impacts following 2 weeks of exposure, although exposure to the mixture suggests increased energy demand as per methionine depletion. Indirect support for increased demand for energy is present in the cardiac proteome as enzymes and enzyme components involved in energy metabolism were enriched. Combined, these findings highlight that no one single pathway is responsible for the development of toxicity following exposure to retene, fluoranthene or their combined binary mixture. Rather, it is likely that exposure induced toxicity through multiple mechanisms.

Ethical approval

Under the European Union Directive 2010/63/EU (*On the Protection of Animals Used for Scientific Purposes*), Chapter 1, Article 1, point 3: no ethical approval is required for in vivo experiments on non-human vertebrate animals deriving their energetic needs from the consumption of yolk.

Funding sources

Academy of Finland project number: 285296, 294066 and 319284 granted to Eeva-Riikka Vehniäinen.

Author contributions

Andreas N. M. Eriksson: Exposure maintenance; sampling; proteomics and metabolomics data analysis; tissue extraction and HPLC analysis; photo-analysis; primary author.

Cyril Rigaud: Experiment design; sampling; exposure maintenance; protein and metabolite extraction; SFS-analysis; Review & Editing.

Anne Rokka: Proteomics;

Morten Skaugen: Proteomics;

Jenna Lihavainen: Metabolomics preparation and principal component analysis; Review & Editing.

Eeva-Riikka Vehniäinen: Group leader; experimental design; Review & Editing.

Declaration of competing interest

The authors declare that they have no known competing financial interests or personal relationships that could have appeared to influence the work reported in this paper.

Acknowledgment

We would like to acknowledge the contribution of laboratory technicians Mervi Koistinen, Emma Pajunen, Hannu Pakkanen and laboratory personnel at Konnevesi research station for technical support. We also like to thank Hanka-Taimen OY fish farm for supplying us with rainbow trout alevins for scientific purposes and research.

Appendix A. Supplementary data

Supplementary data to this article can be found online at <https://doi.org/10.1016/j.scitotenv.2022.154846>.

References

- Ainerua, M.O., Tinwell, J., Kompella, S.N., Sørhus, E., White, K.N., van Dongen, B.E., Shiels, H.A., 2020. Understanding the cardiac toxicity of the anthropogenic pollutant phenanthrene on the freshwater indicator species, the brown trout (*Salmo trutta*): from whole heart to cardiomyocytes. *Chemosphere* 239, 124608. <https://doi.org/10.1016/j.chemosphere.2019.124608>.
- Antkiewicz, D.S., Burns, C.G., Carney, S.A., Peterson, R.E., Heideman, W., 2005. Heart malformation is an early response to TCDD in embryonic zebrafish. *Toxicol. Sci.* 84, 368–377. <https://doi.org/10.1093/toxsci/kfi073>.
- Baquer, N.Z., Hothersall, J.S., McLean, P., 1988. Function and regulation of the pentose phosphate pathway in brain. In: Horecker, B.L., Stadtman, E.R. (Eds.), *Current Topics in Cellular Regulation*. Academic Press, pp. 265–289. <https://doi.org/10.1016/B978-0-12-152829-4.50008-2>.
- Barron, M.G., Heintz, R., Rice, S.D., 2004. Relative potency of PAHs and heterocycles as aryl hydrocarbon receptor agonists in fish. *Mar. Environ. Res.* 58, 95–100. <https://doi.org/10.1016/j.marenvres.2004.03.001>.
- Bateman, R.L., Bhanumoorthy, P., Witte, J.F., McClard, R.W., Grompe, M., Timm, D.E., 2001. Mechanistic inferences from the crystal structure of fumarylacetoacetate hydrolase with a bound phosphorus-based inhibitor. *J. Biol. Chem.* 276, 15284–15291. <https://doi.org/10.1074/jbc.m007621200>.
- Behera, B.K., Das, A., Sarkar, D.J., Weerathunge, P., Parida, P.K., Das, B.K., Thavamani, P., Ramanathan, R., Bansal, V., 2018. Polycyclic aromatic hydrocarbons (PAHs) in inland aquatic ecosystems: perils and remedies through biosensors and bioremediation. *Environ. Pollut.* 241, 212–233. <https://doi.org/10.1016/j.envpol.2018.05.016>.
- Billiard, S.M., Querbach, K., Hodson, P.V., 1999. Toxicity of retene to early life stages of two freshwater fish species. *Environ. Toxicol. Chem.* 18, 2070–2077. <https://doi.org/10.1002/etc.5620180927>.
- Bohne-Kjersem, A., Skadsheim, A., Goksøyr, A., Grøsvik, B.E., 2009. Candidate biomarker discovery in plasma of juvenile cod (*Gadus morhua*) exposed to crude North Sea oil, alkyl phenols and polycyclic aromatic hydrocarbons (PAHs). *Mar. Environ. Res.* 68, 268–277. <https://doi.org/10.1016/j.marenvres.2009.06.016>.
- Bohne-Kjersem, A., Bache, N., Meier, S., Nyhammer, G., Roepstorff, P., Sæle, Ø., Goksøyr, A., Grøsvik, B.E., 2010. Biomarker candidate discovery in Atlantic cod (*Gadus morhua*) continuously exposed to North Sea produced water from egg to fry. *Aquat. Toxicol.* 96, 280–289. <https://doi.org/10.1016/j.aquatox.2009.11.005>.
- Bozinovic, G., Shea, D., Feng, Z., Hinton, D., Sit, T., Oleksiak, M.F., 2021. PAH-pollution effects on sensitive and resistant embryos: integrating structure and function with gene expression. *PLoS ONE* 16, e0249432.
- Colucci-Guyon, E., Portier, M.-M., Dunia, I., Paulin, D., Pourmin, S., Babinet, C., 1994. Mice lacking vimentin develop and reproduce without an obvious phenotype. *Cell* 79, 679–694. [https://doi.org/10.1016/0092-8674\(94\)90553-3](https://doi.org/10.1016/0092-8674(94)90553-3).
- Cox, J., Mann, M., 2008. MaxQuant enables high peptide identification rates, individualized p.p.b.-range mass accuracies and proteome-wide protein quantification. *Nat. Biotechnol.* 26, 1367–1372. <https://doi.org/10.1038/nbt.1511>.
- Cox, J., Neuhauser, N., Michalski, A., Scheltema, R.A., Olsen, J.V., Mann, M., 2011. Andromeda: a peptide search engine integrated into the MaxQuant environment. *J. Proteome Res.* 10, 1794–1805. <https://doi.org/10.1021/pr101065j>.
- Cvetic, C.A., Walter, J.C., 2006. Getting a grip on licensing: mechanism of stable Mcm2-7 loading onto replication origins. *Mol. Cell* 21, 143–144. <https://doi.org/10.1016/j.molcel.2006.01.003>.
- de Soysa, T.Y., Ulrich, A., Friedrich, T., Pite, D., Compton, S.L., Ok, D., Bernardos, R.L., Downes, G.B., Hsieh, S., Stein, R., Lagdameo, M.C., Halvorsen, K., Kesich, L.-R., Barresi, M.J.F., 2012. Macondo crude oil from the Deepwater Horizon oil spill disrupts specific developmental processes during zebrafish embryogenesis. *BMC Biol.* 10, 40. <https://doi.org/10.1186/1741-7007-10-40>.
- Delanghe, J.R., Langlois, M.R., 2001. Hemopexin: a review of biological aspects and the role in laboratory medicine. *Clin. Chim. Acta* 312, 13–23. [https://doi.org/10.1016/S0009-8981\(01\)00586-1](https://doi.org/10.1016/S0009-8981(01)00586-1).
- Dietrich, J.B., 1992. Tyrosine aminotransferase: a transaminase among others? *Cell Mol. Biol.* 38, 95–114.
- Doering, J.A., Tang, S., Peng, H., Eisner, B.K., Sun, J., Giesy, J.P., Wiseman, S., Hecker, M., 2016. High conservation in transcriptomic and proteomic response of white sturgeon to equipotent concentrations of 2,3,7,8-TCDD, PCB 77, and benzo[a]pyrene. *Environ. Sci. Technol.* 50, 4826–4835. <https://doi.org/10.1021/acs.est.6b00490>.
- Doering, J., Hecker, M., Villeneuve, D., Zhang, X., 2019. Adverse Outcome Pathway on Aryl Hydrocarbon Receptor Activation Leading to Early Life Stage Mortality, via Increased COX-2IS. 12. <https://doi.org/10.1787/bd46b538-en>.
- dos Santos, I.F., Ferreira, S.L.C., Domínguez, C., Bayona, J.M., 2018. Analytical strategies for determining the sources and ecotoxicological risk of PAHs in river sediment. *Microchem. J.* 137, 90–97. <https://doi.org/10.1016/j.microc.2017.09.025>.
- Dutta, A., Bell, S.P., 1997. Initiation of DNA replication in eukaryotic cells. *Annu. Rev. Cell Dev. Biol.* 13, 293–332. <https://doi.org/10.1146/annurev.cellbio.13.1.293>.
- Elie, M.R., Choi, J., Nkrumah-Elie, Y., Gonnerman, G.D., Stevens, J.F., Tanguay, R.L., 2015. Metabolomic analysis to define and compare the effects of PAHs and oxygenated PAHs in developing zebrafish. *Environ. Res.* 140, 502–510. <https://doi.org/10.1016/j.envres.2015.05.009>.
- Eriksson, A.N.M., Rigaud, C., Krasnov, A., Wincent, E., Vehniäinen, E.-R., 2022. Exposure to retene, fluoranthene, and their binary mixture causes distinct transcriptomic and apical outcomes in rainbow trout (*Oncorhynchus mykiss*) yolk sac alevins. *Aquat. Toxicol.* 106083. <https://doi.org/10.1016/j.aquatox.2022.106083>.
- Fent, K., Bättscher, R., 2000. Cytochrome P4501A induction potencies of polycyclic aromatic hydrocarbons in a fish hepatoma cell line: demonstration of additive interactions. *Environ. Toxicol. Chem.* 19, 2047–2058. <https://doi.org/10.1002/etc.5620190813>.
- Finkelstein, J.D., Martin, J.J., 2000. Homocysteine. *Int. J. Biochem. Cell Biol.* 32, 385–389. [https://doi.org/10.1016/S1357-2725\(99\)00138-7](https://doi.org/10.1016/S1357-2725(99)00138-7).

- Fukui, Y., Masuda, H., Takagi, M., Takahashi, K., Kiyokane, K., 1997. The presence of h2-calponin in human keratinocyte. *J. Dermatol. Sci.* 14, 29–36. [https://doi.org/10.1016/S0923-1811\(96\)00545-2](https://doi.org/10.1016/S0923-1811(96)00545-2).
- Garner, L.V.T., Brown, D.R., Di Giulio, R.T., 2013. Knockdown of AHR1A but not AHR1B exacerbates PAH and PCB-126 toxicity in zebrafish (*Danio rerio*) embryos. *Aquat. Toxicol.* 142–143, 336–346. <https://doi.org/10.1016/j.aquatox.2013.09.007>.
- Geier, M.C., James Minick, D., Truong, L., Tilton, S., Pande, P., Anderson, K.A., Teeguarden, J., Tanguay, R.L., 2018. Systematic developmental neurotoxicity assessment of a representative PAH superfund mixture using zebrafish. *Toxicol. Appl. Pharmacol.* 354, 115–125. <https://doi.org/10.1016/j.taap.2018.03.029>.
- Grynberg, A., Demaison, L., 1996. Fatty acid oxidation in the heart. *J. Cardiovasc. Pharmacol.* 28 (Suppl. 1), S11–S17. <https://doi.org/10.1097/00005344-19960003-00003>.
- Halliwell, B., Gutteridge, J.M.C., 1985. The importance of free radicals and catalytic metal ions in human diseases. *Mol. Asp. Med.* 8, 89–193. [https://doi.org/10.1016/0098-2997\(85\)90001-9](https://doi.org/10.1016/0098-2997(85)90001-9).
- Hiller, K., Hangebrauk, J., Jäger, C., Spura, J., Schreiber, K., Schomburg, D., 2009. MetaboliteDetector: comprehensive analysis tool for targeted and nontargeted GC/MS based metabolome analysis. *Anal. Chem.* 81, 3429–3439. <https://doi.org/10.1021/ac802689c>.
- Hornung, M.W., Spitsbergen, J.M., Peterson, R.E., 1999. 2,3,7,8-Tetrachlorodibenzo-p-dioxin alters cardiovascular and craniofacial development and function in sac fry of rainbow trout (*Oncorhynchus mykiss*). *Toxicol. Sci.* 47, 40–51. <https://doi.org/10.1093/toxsci/47.1.40>.
- Huang, M., Mesaros, C., Hackfeld, L.C., Hodge, R.P., Zang, T., Blair, I.A., Penning, T.M., 2017. Potential metabolic activation of a representative C4-alkylated polycyclic aromatic hydrocarbon retene (1-methyl-7-isopropyl-phenanthrene) associated with the Deepwater Horizon oil spill in human hepatoma (HepG2) cells. *Chem. Res. Toxicol.* 30, 1093–1101. <https://doi.org/10.1021/acs.chemrestox.6b00457>.
- Hummel, J., Selbig, J., Walther, D., Kopka, J., 2007. The Golm Metabolome Database: a database for GC-MS based metabolite profiling. In: Nielsen, J., Jewett, M.C. (Eds.), *Metabolomics: A Powerful Tool in Systems Biology*. Springer Berlin Heidelberg, Berlin, Heidelberg, pp. 75–95. <https://doi.org/10.1007/978-3-2007-0229-9>.
- Incardona, J.P., 2017. Molecular mechanisms of crude oil developmental toxicity in fish. *Arch. Environ. Contam. Toxicol.* 73, 19–32. <https://doi.org/10.1007/s00244-017-0381-1>.
- Incardona, J.P., Collier, T.K., Scholz, N.L., 2004. Defects in cardiac function precede morphological abnormalities in fish embryos exposed to polycyclic aromatic hydrocarbons. *Toxicol. Appl. Pharmacol.* 196, 191–205. <https://doi.org/10.1016/j.taap.2003.11.026>.
- Incardona, J.P., Day, H.L., Collier, T.K., Scholz, N.L., 2006. Developmental toxicity of 4-ring polycyclic aromatic hydrocarbons in zebrafish is differentially dependent on AH receptor isoforms and hepatic cytochrome P4501A metabolism. *Toxicol. Appl. Pharmacol.* 217, 308–321. <https://doi.org/10.1016/j.taap.2006.09.018>.
- Incardona, J.P., Carls, M.G., Day, H.L., Sloan, C.A., Bolton, J.L., Collier, T.K., Scholz, N.L., 2009. Cardiac arrhythmia is the primary response of embryonic Pacific herring (*Clupea pallasii*) exposed to crude oil during weathering. *Environ. Sci. Technol.* 43, 201–207. <https://doi.org/10.1021/es802270t>.
- Incardona, J.P., Linbo, T.L., Scholz, N.L., 2011. Cardiac toxicity of 5-ring polycyclic aromatic hydrocarbons is differentially dependent on the aryl hydrocarbon receptor 2 isoform during zebrafish development. *Toxicol. Appl. Pharmacol.* 257, 242–249. <https://doi.org/10.1016/j.taap.2011.09.010>.
- Katsumoto, T., Mitsushima, A., Kurimura, T., 1990. The role of the vimentin intermediate filaments in rat 3Y1 cells elucidated by immunoelectron microscopy and computer-graphic reconstruction. *Biol. Cell.* 68, 139–146. [https://doi.org/10.1016/0248-4900\(90\)90299-I](https://doi.org/10.1016/0248-4900(90)90299-I).
- Kim, K.-H., Jahan, S.A., Kabir, E., Brown, R.J.C., 2013. A review of airborne polycyclic aromatic hydrocarbons (PAHs) and their human health effects. *Environ. Int.* 60, 71–80. <https://doi.org/10.1016/j.envint.2013.07.019>.
- Köhle, C., Bock, K.W., 2007. Coordinate regulation of Phase I and II xenobiotic metabolisms by the Ah receptor and Nrf2. *Biochem. Pharmacol.* 73, 1853–1862. <https://doi.org/10.1016/j.bcp.2007.01.009>.
- Larade, K., Storey, K.B., 2004. Accumulation and translation of ferritin heavy chain transcripts following anoxia exposure in a marine invertebrate. *J. Exp. Biol.* 207, 1353. <https://doi.org/10.1242/jeb.00872>.
- Leppänen, H., Oikari, A., 1999. Occurrence of retene and resin acids in sediments and fish bile from a lake receiving pulp and paper mill effluents. *Environ. Toxicol. Chem.* 18, 1498–1505. <https://doi.org/10.1002/etc.5620180723>.
- Leppänen, H., Oikari, A., 2001. Retene and resin acid concentrations in sediment profiles of a lake recovering from exposure to pulp mill effluents. *J. Paleolimnol.* 25, 367–374. <https://doi.org/10.1023/A:1011120426661>.
- Mastrototaro, G., Liang, X., Li, X., Carullo, P., Piroddi, N., Tesi, C., Gu, Y., Dalton, N.D., Peterson, K.L., Poggesi, C., Sheikh, F., Chen, J., Bang, M.-L., 2015. Nebulette knockout mice have normal cardiac function, but show Z-line widening and up-regulation of cardiac stress markers. *Cardiovasc. Res.* 107, 216–225. <https://doi.org/10.1093/cvr/cvv156>.
- Meador, J.P., Nahrgang, J., 2019. Characterizing crude oil toxicity to early-life stage fish based on a complex mixture: are we making unsupported assumptions? *Environ. Sci. Technol.* 53, 11080–11092. <https://doi.org/10.1021/acs.est.9b02889>.
- Meunier, S., Vernos, I., 2012. Microtubule assembly during mitosis – from distinct origins to distinct functions? *J. Cell Sci.* 125, 2805. <https://doi.org/10.1242/jcs.092429>.
- Mitchison, T., Kirschner, M., 1984. Dynamic instability of microtubule growth. *Nature* 312, 237–242. <https://doi.org/10.1038/312237a0>.
- Nogales, E., 2000. Structural insights into microtubule function. *Annu. Rev. Biochem.* 69, 277–302. <https://doi.org/10.1146/annurev.biochem.69.1.277>.
- OECD, 2013. Test No. 236: Fish Embryo Acute Toxicity (FET) Test. OECDiLibrary <https://doi.org/10.1787/9789264203709-en>.
- Oliver, I.T., 1955. A spectrophotometric method for the determination of creatine phosphokinase and myokinase. *Biochem. J.* 61, 116–122. <https://doi.org/10.1042/bj0610116>.
- Olsvik, P.A., Lie, K.K., Nordtug, T., Hansen, B.H., 2012. Is chemically dispersed oil more toxic to Atlantic cod (*Gadus morhua*) larvae than mechanically dispersed oil? A transcriptional evaluation. *BMC Genomics* 13, 702. <https://doi.org/10.1186/1471-2164-13-702>.
- Page, D.S., Boehm, P.D., Douglas, G.S., Bence, A.E., Burns, W.A., Mankiewicz, P.J., 1999. Pyrogenic polycyclic aromatic hydrocarbons in sediments record past human activity: a case study in Prince William Sound, Alaska. *Mar. Pollut. Bull.* 38, 247–260. [https://doi.org/10.1016/S0025-326X\(98\)00142-8](https://doi.org/10.1016/S0025-326X(98)00142-8).
- Paramio, J.M., Jorcano, J.L., 2002. Beyond structure: do intermediate filaments modulate cell signalling? *Bioessays* 24, 836–844. <https://doi.org/10.1002/bies.10140>.
- Pasparakis, C., Esbaugh, A.J., Burggren, W., Grosell, M., 2019. Physiological impacts of Deepwater Horizon oil on fish. *Comp. Biochem. Physiol. C: Toxicol. Pharmacol.* 224, 108558. <https://doi.org/10.1016/j.cbpc.2019.06.002>.
- Rigaud, C., Eriksson, A., Krasnov, A., Wincent, E., Pakkanen, H., Lehtivuori, H., Ihalainen, J., Vehniäinen, E.-R., 2020a. Retene, pyrene and phenanthrene cause distinct molecular-level changes in the cardiac tissue of rainbow trout (*Oncorhynchus mykiss*) larvae, part 1 – transcriptomics. *Sci. Total Environ.* 745, 141031. <https://doi.org/10.1016/j.scitotenv.2020.141031>.
- Rigaud, C., Eriksson, A., Rokka, A., Skaugen, M., Lihavainen, J., Keinänen, M., Lehtivuori, H., Vehniäinen, E.-R., 2020b. Retene, pyrene and phenanthrene cause distinct molecular-level changes in the cardiac tissue of rainbow trout (*Oncorhynchus mykiss*) larvae, part 2 – proteomics and metabolomics. *Sci. Total Environ.* 746, 141161. <https://doi.org/10.1016/j.scitotenv.2020.141161>.
- Sawicki, K.T., Hsiang-Chun, Chang, Hossein, A., 2015. Role of heme in cardiovascular physiology and disease. *J. Am. Heart Assoc.* 4, e001138. <https://doi.org/10.1161/JAHA.114.001138>.
- Scott, J.A., Hodson, P.V., 2008. Evidence for multiple mechanisms of toxicity in larval rainbow trout (*Oncorhynchus mykiss*) co-treated with retene and α -naphthoflavone. *Aquat. Toxicol.* 88, 200–206. <https://doi.org/10.1016/j.aquatox.2008.04.007>.
- Scott, J.A., Incardona, J.P., Pelkki, K., Shepardson, S., Hodson, P.V., 2011. AhR2-mediated, CYP1A-independent cardiovascular toxicity in zebrafish (*Danio rerio*) embryos exposed to retene. *Aquat. Toxicol.* 101, 165–174. <https://doi.org/10.1016/j.aquatox.2010.09.016>.
- Sequeira, V., Nijenkamp, L.L.A.M., Regan, J.A., van der Velden, J., 2014. The physiological role of cardiac cytoskeleton and its alterations in heart failure. 1838, 700–722. <https://doi.org/10.1016/j.bbame.2013.07.011> Reciprocal influences between cell cytoskeleton and membrane channels, receptors and transporters.
- Sørhus, E., Incardona, J.P., Furmanek, T., Goetz, G.W., Scholz, N.L., Meier, S., Edvardsen, R.B., Jentoft, S., 2017. Novel adverse outcome pathways revealed by chemical genetics in a developing marine fish. *eLife* 6, e20707. <https://doi.org/10.7554/eLife.20707>.
- Sørhus, E., Meier, S., Donald, C.E., Furmanek, T., Edvardsen, R.B., Lie, K.K., 2021. Cardiac dysfunction affects eye development and vision by reducing supply of lipids in fish. *Sci. Total Environ.* 800, 149460. <https://doi.org/10.1016/j.scitotenv.2021.149460>.
- Stanton, R.C., 2012. Glucose-6-phosphate dehydrogenase, NADPH, and cell survival. *IUBMB Life* 64, 362–369. <https://doi.org/10.1002/iub.1017>.
- Tang, J., Hu, G., Hanai, J., Yadlapalli, G., Lin, Y., Zhang, B., Galloway, J., Bahary, N., Sinha, S., Thisse, B., Thisse, C., Jin, J.-P., Zon, L.I., Sukhatme, V.P., 2006. A critical role for calponin 2 in vascular development. *J. Biol. Chem.* 281, 6664–6672. <https://doi.org/10.1074/jbc.m506991200>.
- Tanguay, R.L., Andreasen, E.A., Walker, M.K., Peterson, R.E., 2003. Dioxin toxicity and aryl hydrocarbon receptor signaling in fish. *Dioxins and Health*. Wiley Online Books, pp. 603–628. <https://doi.org/10.1002/0471722014.ch15>.
- Tolosano, E., Altruda, F., 2002. Hemopexin: structure, function, and regulation. *DNA Cell Biol.* 21, 297–306. <https://doi.org/10.1089/104454902753759717>.
- Troisi, G., Borjesson, L., Bexton, S., Robinson, I., 2007. Biomarkers of polycyclic aromatic hydrocarbon (PAH)-associated hemolytic anemia in oiled wildlife. *Environ. Res.* 105, 324–329. <https://doi.org/10.1016/j.envres.2007.06.007>.
- Tyanova, S., Temu, T., Sinitcyn, P., Carlson, A., Hein, M.Y., Geiger, T., Mann, M., Cox, J., 2016. The Perseus computational platform for comprehensive analysis of (prote)omics data. *Nat. Methods* 13, 731–740. <https://doi.org/10.1038/nmeth.3901>.
- Uyeda, K., 1979. Phosphofructokinase. *Adv. Enzymol. Relat. Areas Mol. Biol.* 193–244. <https://doi.org/10.1002/9780470122938.ch4>.
- Van Tiem, L.A., Di Giulio, R.T., 2011. AHR2 knockdown prevents PAH-mediated cardiac toxicity and XRE- and ARE-associated gene induction in zebrafish (*Danio rerio*). *Toxicol. Appl. Pharmacol.* 254, 280–287. <https://doi.org/10.1016/j.taap.2011.05.002>.
- Vehniäinen, E.-R., Bremer, K., Scott, J.A., Juntila, S., Laiho, A., Gyenesi, A., Hodson, P.V., Oikari, A.O.J., 2016. Retene causes multifunctional transcriptomic changes in the heart of rainbow trout (*Oncorhynchus mykiss*) embryos. *Environ. Toxicol. Pharmacol.* 41, 95–102. <https://doi.org/10.1016/j.etap.2015.11.015>.
- Vehniäinen, E.-R., Haverinen, J., Vehniäinen, E.-R., 2019. Polycyclic aromatic hydrocarbons phenanthrene and retene modify the action potential via multiple ion currents in rainbow trout *Oncorhynchus mykiss* cardiac myocytes. *Environ. Toxicol. Chem.* 38, 2145–2153. <https://doi.org/10.1002/etc.4530>.
- Vernier, J.M., 1977. *Chronological Table of the Embryonic Development of Rainbow Trout, Salmo Gairdneri Rich.* 1836. Fisheries and Marine Service. Translation Series. Department of the Environment, Fisheries and Marine Service, Pacific Biological Station, Canada.
- Villalobos, S.A., Papoulias, D.M., Meadows, J., Blankenship, A.L., Pastva, S.D., Kannan, K., Hinton, D.E., Tillitt, D.E., Giesy, J.P., 2000. Toxic responses of medaka, D-r strain, to polychlorinated naphthalene mixtures after embryonic exposure by in ovo nanoinjection: a partial life-cycle assessment. *Environ. Toxicol. Chem.* 19, 432–440. <https://doi.org/10.1002/etc.5620190224>.
- Vogel, C., Marcotte, E.M., 2012. Insights into the regulation of protein abundance from proteomic and transcriptomic analyses. *Nat. Rev. Genet.* 13, 227–232. <https://doi.org/10.1038/nrg3185>.
- Wassenberg, D., Di Giulio, R., 2004a. Synergistic embryotoxicity of polycyclic aromatic hydrocarbon aryl hydrocarbon receptor agonists with cytochrome P4501A inhibitors in

- Fundulus heteroclitus. *Environ. Health Perspect.* 112, 1658–1664. <https://doi.org/10.1289/ehp.7168>.
- Wassenberg, D., Di Giulio, R., 2004b. Teratogenesis in *Fundulus heteroclitus* embryos exposed to a creosote-contaminated sediment extract and CYP1A inhibitors. *Mar. Environ. Res.* 58, 163–168. <https://doi.org/10.1016/j.marenvres.2004.03.012>.
- Weiss, H.J., Sussman, I.I., Hoyer, L.W., 1977. Stabilization of factor VIII in plasma by the von Willebrand factor. Studies on posttransfusion and dissociated factor VIII and in patients with von Willebrand's disease. *J. Clin. Invest.* 60, 390–404. <https://doi.org/10.1172/JCI108788>.
- Wickström, K., Tolonen, K., 1987. The history of airborne polycyclic aromatic hydrocarbons (PAH) and perylene as recorded in dated lake sediments. *Water Air Soil Pollut.* 32, 155–175. <https://doi.org/10.1007/BF00227691>.
- Willett, K.L., Randerath, K., Zhou, G.-D., Safe, S.H., 1998. Inhibition of CYP1A1-dependent activity by the polynuclear aromatic hydrocarbon (PAH) fluoranthene. *Biochem. Pharmacol.* 55, 831–839. [https://doi.org/10.1016/S0006-2952\(97\)00561-3](https://doi.org/10.1016/S0006-2952(97)00561-3).
- Williamson, J.R., 1979. Mitochondrial function in the heart. *Annu. Rev. Physiol.* 41, 485–506. <https://doi.org/10.1146/annurev.ph.41.030179.002413>.
- Wills, L.P., Zhu, S., Willett, K.L., Di Giulio, R.T., 2009. Effect of CYP1A inhibition on the biotransformation of benzo[a]pyrene in two populations of *Fundulus heteroclitus* with different exposure histories. *Aquat. Toxicol.* 92, 195–201. <https://doi.org/10.1016/j.aquatox.2009.01.009>.
- Yue, M.S., Martin, S.E., Martin, N.R., Taylor, M.R., Plavicki, J.S., 2021. 2,3,7,8-Tetrachlorodibenzo-p-dioxin exposure disrupts development of the visceral and ocular vasculature. *Aquat. Toxicol.* 234, 105786. <https://doi.org/10.1016/j.aquatox.2021.105786>.
- Zhou, Y., Zhou, B., Pache, L., Chang, M., Khodabakhshi, A.H., Tanaseichuk, O., Benner, C., Chanda, S.K., 2019. Metascape provides a biologist-oriented resource for the analysis of systems-level datasets. *Nat. Commun.* 10, 1523. <https://doi.org/10.1038/s41467-019-09234-6>.
- Zimmerman, T.S., Edgington, T.S., 1973. Factor VIII coagulant activity and factor VIII-like antigen: independent molecular entities. *J. Exp. Med.* 138, 1015–1020. <https://doi.org/10.1084/jem.138.4.1015>.
- Zodrow, J.M., Tanguay, R.L., 2003. 2,3,7,8-Tetrachlorodibenzo-p-dioxin inhibits zebrafish caudal fin regeneration. *Toxicol. Sci.* 76, 151–161. <https://doi.org/10.1093/toxsci/kfg205>.